



*The Abdus Salam
International Centre for Theoretical Physics*



2052-12

Summer College on Plasma Physics

10 - 28 August 2009

Turbulent transport in fusion plasmas, effects of toroidicity and fluid closure

Jan Weiland
*Chalmers University of Technology
Sweden*

Turbulent transport in fusion plasmas, effects of toroidicity and fluid closure

Jan Weiland

Department of Radio and Space Science
Chalmers University and EURATOM-VR Association

**Presentation at Summer College on Plasma Physics, ICTP Trieste
August 10 – 14 2009**

GENERAL ASPECTS OF TRANSPORT

Transport in tokamaks is **dominated** by low frequency turbulence.

Typical correlation lengths are of the order $k\rho \approx 0.3$ in agreement with simulations of **drift wave turbulence**

Typical frequencies are about *two orders of magnitude below the ion cyclotron frequency*

Turbulence levels are of the order $e\phi/T \approx 0.01$ which is in agreement with the mixing length estimate (Kadomtsev, Plasma turbulence Academic press 1965)

Saturation level

The mixing length level is given by a balance between linear ExB convection (usually a part of the instability mechanism) and the nonlinear ExB convection which gives transport. Thus:

$$\mathbf{v}_E \cdot \nabla n = \mathbf{v}_E \cdot \nabla \delta n$$

Where n is the background density and δn is the perturbation in density. This leads to the saturation level (*Kadomtsev 1965*):

$$\frac{\partial n}{n} = \frac{1}{k_r L_n} \quad (1)$$

Non-Markovian mixing-length

The mixing length level is actually the maximum saturation level. The balance between the linear growth and nonlinear convection gives a more direct estimate:

$$\gamma \delta T = \mathbf{v}_E \cdot \nabla \delta T$$

Taking space variations as inverse correlation lengths, k , we get

$$\frac{e\phi}{T_e} = \frac{\gamma}{k_\theta c_s k_r \rho_s} = \frac{\gamma}{\omega_*} \frac{1}{k_r L_n} \quad (2)$$

Saturation

The situation is well illustrated by Fig 1

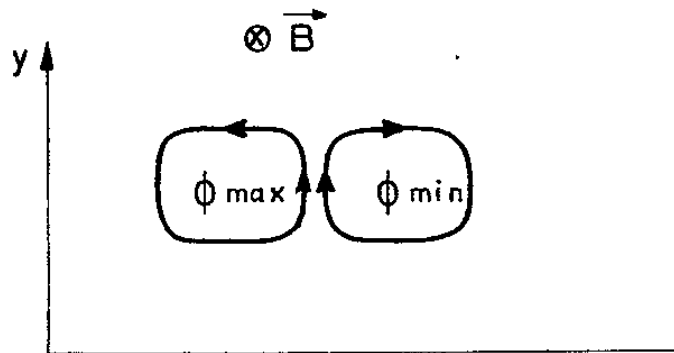


Fig 1

The mixing length level (1) corresponds to convection going the full way around while the result (2) includes rocking due to the real eigenfrequency

Saturation

This is seen from the expression for the convective perturbation

$$\delta n = \xi \cdot \nabla n \quad \text{where} \quad \mathbf{v}_E = \frac{d}{dt} \xi \quad (3)$$

ξ is the ExB displacement

Now, combining (3) with (1) gives:

$$|\xi| = \frac{1}{k_r} \quad (4)$$

and, combining (3) with (2) gives:

$$|\xi| = \frac{1}{k_r} \frac{\gamma}{|\omega|} \quad (5)$$

Flux

$$\Gamma = \langle V_{E_r} \delta T \rangle = -\chi \frac{\partial T}{\partial r} \quad \delta T = \xi \cdot \nabla T$$

Diffusivity

Now entering the displacements (4) and (5) into the convective flux and using Ficks law we get:

$$\text{From 4} \quad D = \gamma / k_r^2 \quad (6)$$

(Kadomtsev estimate)

$$\text{From 5} \quad D = \frac{\gamma^3 / k_r^2}{\omega_r^2 + \gamma^2} \quad (7)$$

The result (7) was first obtained in a somewhat more general form in J. Weiland and H. Nordman, Proc. Varenna-Lausanne workshop, Chexbres 1988, p451 using the type of derivation outlined here. Later a more rigorous derivation was made in A. Zagorodny and J. Weiland, Phys. Plasmas **6**, 2359 (1999).

Turbulent transport

When we have many waves we have to estimate their total effect. The estimate (6) was first suggested by Kadomtsev in his book Plasma turbulence, Academic, 1965.

Kadomtsev also argued that this would give the total transport when k_r is chosen as the inverse correlation length and γ is the corresponding growthrate. (Nedospasov, Phys. Plasmas 16, 060501 (2009))

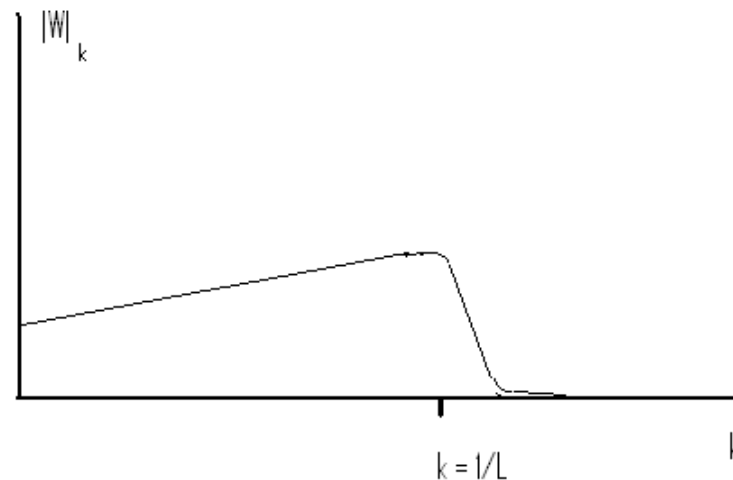
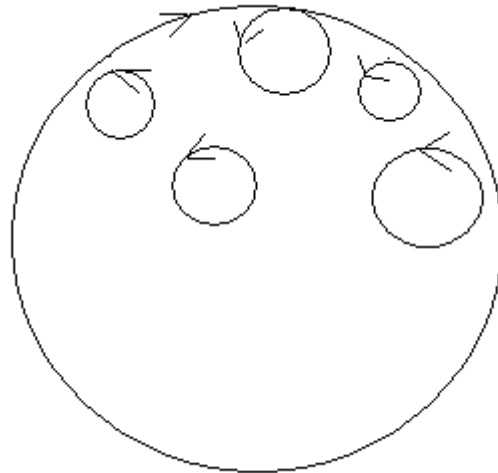


Fig 2

Dominance of smaller eddies in correlation length



$$\mathbf{V}_E = \frac{1}{B} (\hat{e} \times \nabla \phi)$$

Smaller eddies have faster rotation for the same field strength ($\mathbf{E} \times \mathbf{B}$ rotation). They tear apart larger eddies and reduce the correlation length

Correlation length

The correlation length L is defined as the scale length of the turbulence space dependence. The Fourier representation of the space variation is:

$$\phi = \sum \phi_{\mathbf{k}} e^{i\mathbf{k}\cdot\mathbf{r}}$$

and its space variation is:

$$\frac{\partial \phi_{\mathbf{k}}}{\partial \mathbf{r}} = i \sum \mathbf{k} \phi_{\mathbf{k}} e^{i\mathbf{k}\cdot\mathbf{r}}$$

Thus long wavelengths contribute little to the space variation. We thus expect the inverse correlation length to be located according to Fig 2

Boundary conditions

While the saturation level (4) has the character of maximum possible level (wave braking limit), the level (5) was obtained by balancing linear growth and nonlinear damping. This means that *the nonlinearity is entirely stabilizing*

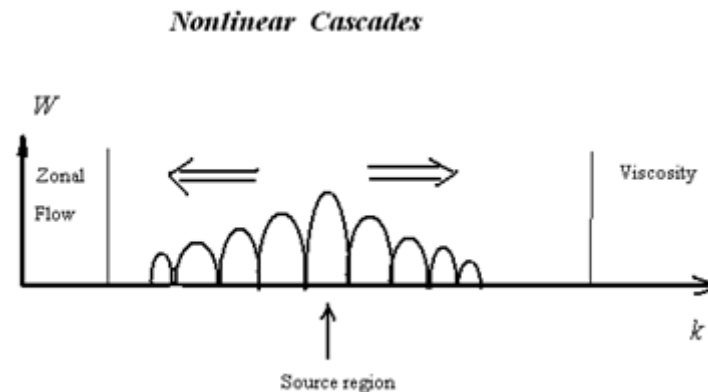


Fig 3

Entirely stabilizing nonlinearity excludes reflections in k-space from the boundaries in k

Absorbing boundaries in k-space

Since (6) is obtained as a limiting case of (7) it must also be restricted to absorbing boundaries in k-space

However, another way of looking at it is that there is a *natural source* at the fastest growing mode. *Reflections* In k-space would introduce *another source* leading to an *effective source* with an *intermediate* correlation length

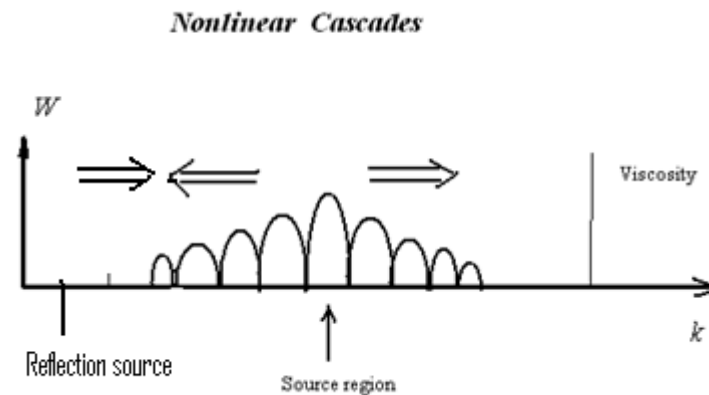


Fig 4

Stabilizing mechanisms

Absorbing mechanisms are mainly

For large k : Viscosity

For small k : Zonal flows

Since zonal flows are more efficient in absorbing turbulence the longer the wavelength gets, turbulence codes have to use a ***sufficiently large box size*** in order to have absorbing boundary for long wavelength

For our reactive fluid model the required box size was about half the radius (Dastgeer et. al. Phys. Plasmas **9**, 1565 (2002)).

Ion thermal conductivity

With our reactive fluid model, which includes the perpendicular fluid resonance, and assuming Boltzmann electrons we then get:

$$\chi_i = \frac{1}{\eta_i} \left(\eta_i - \frac{2}{3} - \frac{10}{9\tau} \varepsilon_n \right) \frac{\gamma^3 / k_r^2}{\left(\omega_r - \frac{5}{3} \omega_{Di} \right)^2 + \gamma^2} \quad (8)$$

In addition to the non-Markovian feature included in (7), (8) also includes off diagonal fluxes and a Doppler shift due to the magnetic drift. This is the thermal conductivity obtained in Weiland, Nordman, Chexbres 1988 and has the same normalization as (7) and accordingly also as (6) as suggested by Kadomtsev.

Turbulence simulations

The result (8) was confirmed within 20% by turbulence simulations for a Cartesian geometry in J. Weiland and H. Nordman, Proc. Varenna-Lausanne workshop, Chexbres 1988 p. 451, and H. Nordman and J. Weiland, Nuclear Fusion **29**, 251 (1989) and for the Cyclone parameters in a Connor Hastie Taylor equilibrium in Dastgeer Shaikh, Sangeeta Mahajan and Jan Weiland, Phys Plasmas **9**, 1565 (2002).

Kadomtsev's estimate

Our result (8) turns into Kadomtsev's estimate when non-Markovian and off diagonal effects are ignored. This usually does not change the order of magnitude.

It is interesting to compare Kadomtsev's estimate with more recent results. While our diffusivity is somewhat smaller than the Kadomtsev prediction the kinetic growth rate is smaller. For the Cyclone case the results are, in fact, close. (Dimitis et.al. Phys Plasmas **7**, 969 (2000).)

The Cyclone base case

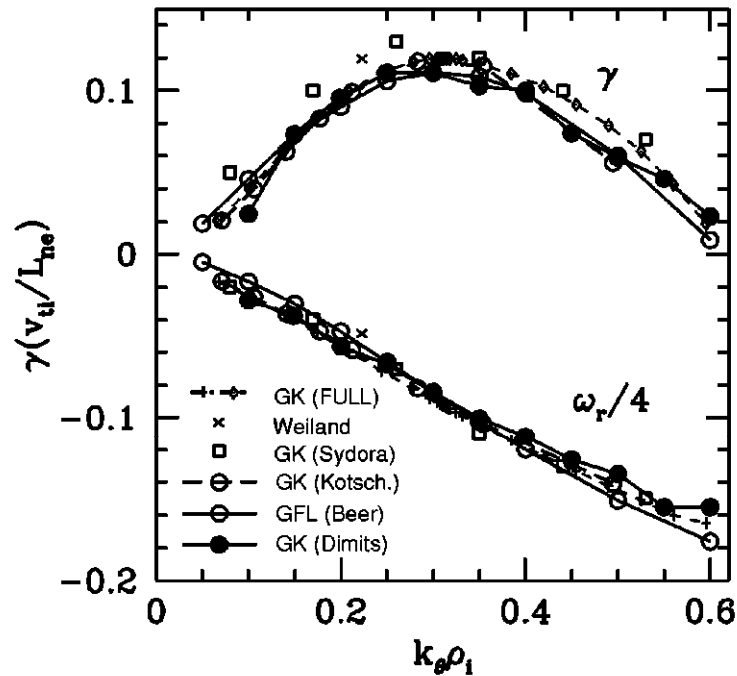


Fig 5 Comparison of linear models for DIII-D 81499 (H-mode) at half radius

FIG. 1. γ and ω_r vs k_θ for the Sydora (global) and Dimits (flux-tube) nonlinear gyrokinetic codes, for the Kotschenreuther and Rewoldt (FULL) linear gyrokinetic codes, the Beer nonlinear gyrofluid code, and the Weiland fluid calculation.

Linear growthrates Maximum at $k\rho_i = 0.3$ (here $\rho_i = \rho_s$)

The Cyclone basecase

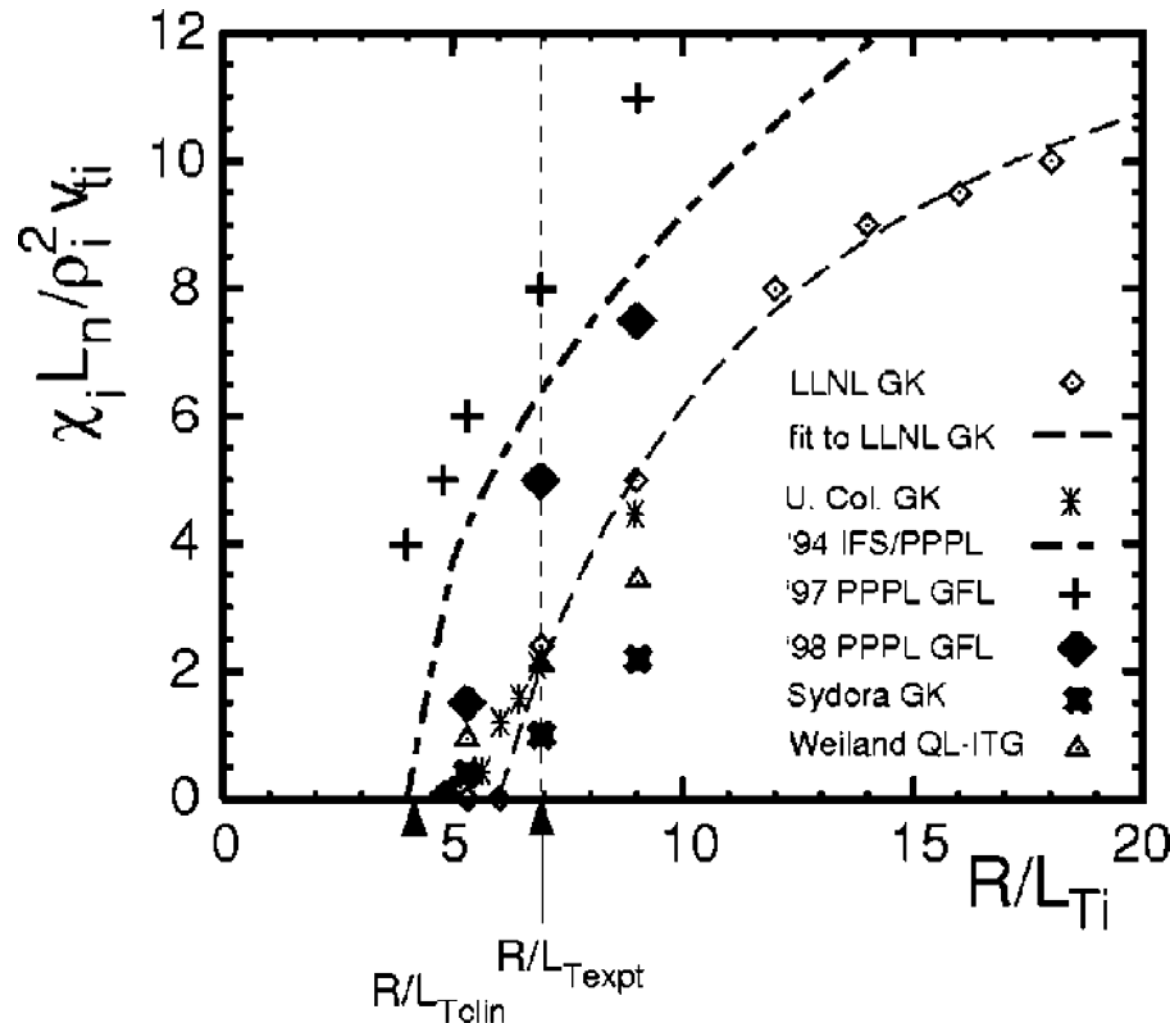


Fig 6 Comparison of transport models for DIII-D 81499 (H-mode) at half radius

Transport level

To recover the IFS-PPPL result for the Cyclone basecase with the Kadomtsev formula and the kinetic growthrate requires a correlation length about 3 times the wavelength of the fastest growing mode

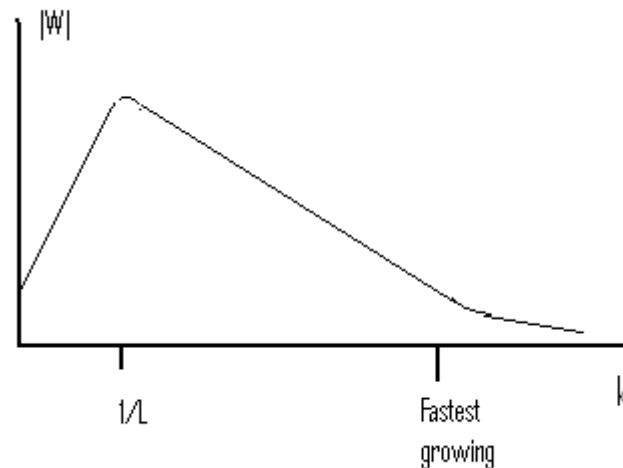


Fig 7

Effects of toroidicity

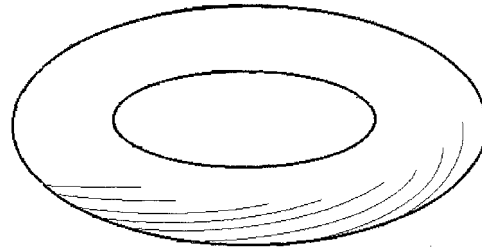
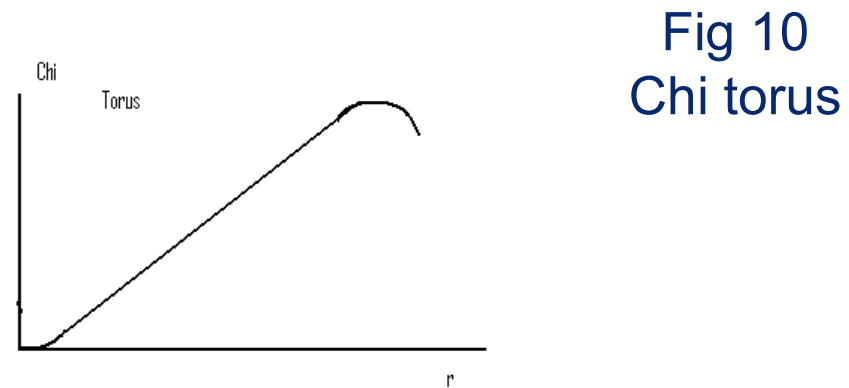
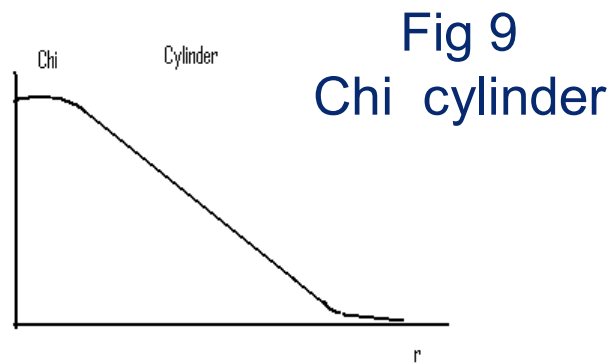


Fig 8

Toroidal effects are very fundamental since *they represent the third dimension in which the magnetic field does not confine the plasma*

Toroidal effects make Chi grow with radius in a tokamak



Radial growth of Chi

The toroidal effects (from the fluid closure) in Eq (8) are responsible for the radial growth of Chi.

The fact that toroidal effects cause the radial growth was also found in nonlinear kinetic simulations by M.J. LeBrun, et al. (Phys. Fluids **B5**, 752 (1993)).

Electron trapping further emphasizes the radial growth.

Several transport channels

We have above focused on ion thermal transport. Several other channels such as electron thermal transport, multiple species particle transport and momentum transport can be described in similar ways. Of particular present interest are:

Particle transport

Momentum transport

Particle transport

A particle pinch has for a long time been needed to understand tokamak transport (Wagner and Stroth, Plasma Phys. Control. Fusion **35**, 1321 (1993)). A particle pinch of the right magnitude was obtained by a reactive fluid model including the perpendicular fluid resonance due to toroidicity. (L. Garzotti et. al. Nuclear Fusion **43**, 1829 (2003))

The **particle pinch** is particularly sensitive to the fluid closure and **quasilinear kinetic models** usually get a **too weak** particle pinch.

This is in agreement with theory indicating that **strongly nonlinear effects lead to a reactive fluid closure.**

Momentum transport

Momentum transport is needed to calculate shear flows
In a plasma. These may stabilize instabilities (B. Lehnert
Phys. Fluids **9**, 1367 (1966))

The fluid momentum equation is written:

$$m_i N_i \left(\frac{\partial}{\partial t} + \vec{U}_i \cdot \vec{\nabla} \right) \vec{U}_i = -\vec{\nabla} P_i - \vec{\nabla} \cdot \vec{\pi}_i + e N_i (\vec{E} + \vec{U}_i \times \vec{B}) \quad (9)$$

where U is the fluid velocity and π is the stress tensor

We will here only consider the toroidal component
which is well approximated by the parallel.

Toroidal momentum

Again **toroidal effects** turn out to be very important!

We can proceed along *two different routs*. Either we use **fluid** equations like (9) or we use **gyrofluid** equations. Fluid equations are obtained by taking moments of the **Vlasov** equation while gyrofluid equations are obtained by taking moments of the **gyrokinetic** equation.

At first we might not expect toroidal effects, other than an effect on the parallel wavenumber to enter the parallel momentum equation.

However, the parallel and perpendicular dynamics are, in fact, coupled through toroidal effects!

Doppler shift

The first inclusion of magnetic drift effects in the parallel momentum equation seems to have been in connection with the derivation of gyrofluid equations by Waltz, Hammett and Dominguez (Phys Fluids **B4**, 3138 (1992)). Toroidal effects there enter as a convective magnetic drift term with a coefficient 2.

$$\omega \rightarrow \omega - 2\omega_D \quad (10)$$

This toroidal effect was first included for momentum transport by Peeters, Angioni and Strinzi, (Phys. Rev. Lett. **98**, 265003 (2007)) and by Hahm et. al. (Phys. Plasmas **14**, 072302 (2007)).

Doppler shift cont.

Since the magnetic drift is not a fluid drift, the Doppler shift has to come from the stress tensor in the fluid derivation (**fluid and gyrofluid equations have to give the same result!**).

This was verified by Strinzi, Peeters and Weiland (Physics of Plasmas **15**, 044502 (2008))

Diagonal transport element

The Diagonal transport element is obtained from ExB convective momentum perturbation in the background gradient just as for density and temperature transport

$$\chi_{\phi D} = \frac{\gamma^3 / k_r^2}{(\omega_r - 2\omega_D)^2 + \gamma^2} \quad (11)$$

The corresponding ion thermal conductivity is just the diagonal part of (8).

$$\chi_{iD} = \frac{\gamma^3 / k_r^2}{(\omega_r - \frac{5}{3}\omega_D)^2 + \gamma^2} \quad (12)$$

Prandtl number

The Prandtl number is defined as:

$$\text{Pr} = \chi_\phi / \chi_i \quad (13)$$

It has traditionally been assumed to be close to 1. As seen from (11) and (12) this will usually be well fulfilled for the diagonal components except near marginal stability since there

$$\omega_r = \frac{5}{3} \omega_{Di} \quad (14)$$

Prandtl number

The ITG mode is close to marginal stability near the axis so there the *diagonal Prandtl number* is substantially below 1.

Since the convective flux is usually stronger for momentum than for ion temperature transport, the *effective Prandtl number* is typically between 0.2 and 0.5.

Convective transport of toroidal momentum

The convective transport of toroidal momentum has been derived from gyrofluid equations by Hahm et.al. Phys Plasmas **14**, 072302 (2007); Peeters et. al. Phys. Rev. Lett **98**, 265003 (2007)

We will here follow the recent formulation from fluid equations by Weiland et.al. Nuclear Fusion **49**, 065033 (2009)

Fluid derivation of convective toroidal momentum transport

$$m_i N_i \left(\frac{\partial}{\partial t} + \vec{U}_i \cdot \vec{\nabla} \right) \vec{U}_i = -\vec{\nabla} P_i - \vec{\nabla} \cdot \vec{\pi}_i + e N_i (\vec{E} + \vec{U}_i \times \vec{B})$$

The stress tensor π is taken from Classen et. al. Phys. Plasmas **7**, 3699 (2000). It has the general symmetry property

$$\vec{\pi} = \alpha\beta + \beta\alpha$$

Convective diamagnetic effects are cancelled by the stress tensor

Convective momentum transport

The linear perturbation of parallel momentum is then

$$m_i N_i \left(\frac{\partial}{\partial t} + 2\vec{U}_{Di} \cdot \vec{\nabla} \right) \delta u_{\parallel} = - \left[\hat{e}_{\parallel} \cdot \nabla + U_{\parallel 0} \frac{m_i \vec{U}_{Di} \cdot \nabla}{T_i} \right] (\delta p_i + e N_i \phi) \quad (15)$$

We here again notice the convective magnetic drift contribution . The new part is the last magnetic drift term. It adds to the parallel operator and this is the reason for symmetry breaking. As we know the plasma flow introduces unsymmetry also in the parallel operator. Taking Boltzmann density perturbation gives us a pinch of the form $2\omega_D U_{\parallel} \phi$. This term corresponds to the **Coriolis pinch** of Peeters, Angioni and Strinzi. This term was also recovered by Hahm (we have only a factor 2 because we use the total magnetic drift).

Symmetry breaking effects

The linear velocity perturbation in Fourier space is

$$\delta u_{\parallel} = \frac{k_{\parallel} c_s^2 - \omega_{De} U_{\parallel 0}}{\omega - 2\omega_{Di}} \left(\frac{1}{\tau} \frac{\delta p_i}{P_i} + \frac{e\Phi}{T_e} \right) \quad (16)$$

The corresponding flux is calculated as:

$$\Gamma = \langle \delta v_{\parallel} v_{Er} \rangle \quad (17)$$

Eigenvalue problem

The eigenvalue problem with a sheared flow is primarily in the radial direction. We use the direct method of Taylor and Wilson (PPCF **38**, 1999 (1996)) and the eigenvalue solution by Davydova and Weiland (Physics of Plasmas **7**, 243 (2000)). The result is:

$$k_{\parallel} = -\frac{1}{qR} \frac{0.5(\varpi + \frac{5}{3})K + h(\varpi - \varpi_{rk})\kappa_1}{\varpi(1 + \frac{5}{3}) + \frac{1}{\varepsilon_n \tau} (\eta_i - \frac{2}{3}) + \frac{5}{3\tau} (1 + \frac{1}{\tau})} \quad (18a)$$

where

$$K = \left(\frac{sk_{\theta}^2 Rq}{\Omega_{ci}} \frac{dU_{\parallel 0}}{dy} + KS \right) \frac{\omega}{\omega - 2\omega_{Di}} \quad (18b)$$

and

$$KS = 2 * q * k_{\theta} \rho_s \tau^2 \frac{U_{\parallel 0}}{c_s} \quad (18c)$$

Symmetry breaking

Here KS is due to curvature while the coefficient κ is linear in the flowshear. Thus we see that the parallel wavenumber is generated by flowshear and toroidicity. Also the toroidicity effect includes the background flow.

Preliminary simulations indicate that the right level of momentum transport is obtained with this model. No additional fudge factor has been introduced

Conclusions

We have shown the importance of **toroidal effects** for tokamak transport of temperature, density and momentum

All of these but in particular particle transport depend strongly on the fluid closure

The fluid closure depends strongly on toroidal effects.

Early estimates of transport by Kadomtsev are amazingly good